processes

MDPI

Article

Green Synthesis of 3-Hydroxybutyraldehyde from Acetaldehyde Catalyzed by La-Ca-Modified MgO/Al_2O_3

Hailun Ren [1] and Weihong Li [2,*]

[1] Tianjin Ren'ai College, Tianjin 301636, China; hlren@tju.edu.cn
[2] Tianjin Shuang'an Labor Protection Rubber Co., Ltd., Tianjin 300221, China
* Correspondence: weihli@tju.edu.cn

Abstract: 3-hydroxybutyraldehyde (3-HBA) is mainly employed to synthesize 1,3-BDO (1,3-butanediol), which is one of the most important components in cosmetics moisturizers. In this study, a series of composite oxide catalysts were prepared by bringing alkaline earth metal Ca and rare earth metal La to the composite oxide MgO/Al_2O_3, which were made through the co-precipitation method. These catalysts were applied in the synthesis of 3-HBA through acetaldehyde (AcH) condensation. The structure, texture, and acidic properties of these catalysts were characterized using various characterization methods, and the effects of catalyst composition, reaction temperature, reaction pressure, and residence time on the conversion of AcH were investigated as well. The results showed that the introduction of Ca and La weakened the acidic property and enhanced the basic property, which favored the AcH condensation to synthesize 3-HBA. At a temperature of 20 °C, pressure of 200 kPa, and residence time of 70 min, 0.5%La-2.3%Ca-2MgO/Al_2O_3 exhibited a better catalytic activity, and the conversion of AcH reached 95.89%. The selectivity and yield of 3-HBA were 92.08% and 88.30%, respectively. The stability test indicated that the high AcH conversion could be maintained for 5 h.

Keywords: composite oxides; acetaldehyde; condensation catalyst; 3-hydroxybutyraldehyde

Citation: Ren, H.; Li, W. Green Synthesis of 3-Hydroxybutyraldehyde from Acetaldehyde Catalyzed by La-Ca-Modified MgO/Al_2O_3. *Processes* **2022**, *10*, 1302. https://doi.org/10.3390/pr10071302

Academic Editor: Francesco Parrino

Received: 6 April 2022
Accepted: 28 June 2022
Published: 1 July 2022

1. Introduction

1,3-butanediol (1, 3-BDO) is one of the important components of cosmetics moisturizers. Not only does it have minor skin irritation but it also has good bacteriostatic action. Being one of the indispensable raw materials in the cosmetics industry, it is being widely used in the production of cosmetic water, ointment, toothpaste, and other daily chemicals [1–3].

The main synthesis methods of 1, 3-BDO include the biological method, isobutylene-formaldehyde method, propylene-formaldehyde condensation hydrolysis method, acetaldehyde (AcH) condensation hydrogenation method, acrolein-2,2-dimethyl-1,3-propanediol method, and laser irradiation ethanol method [4–9]. Considering the factors such as raw material source, product yield, process difficulty, operation cost, and fixed investment, the AcH condensation hydrogenation method is most suitable for industrialization. The specific process goes as follows: under the action of an alkaline catalyst, AcH is first condensed to 3-hydroxybutyraldehyde (3-HBA) and then hydrogenated to 1,3-BDO. Aldol condensation is an important C–C-bond-forming reaction in organic chemistry, and 3-HBA could be synthesized via the aldol condensation of AcH. However, the aldol condensation reaction was often performed in a homogeneous base (NaOH, KOH, or $Ca(OH)_2$)-catalyzed mixture, which can lead to reactor corrosion and the production of salt wastes [10–13]. The large number of wastewater and waste salts formed in the process are hostile to the environment and cause additional treatment burden [10–13]. Nevertheless, it is not easy to control the reaction process of AcH condensation. If the catalyst and process conditions are unfitting, a large number of by-products such as 2-butenal (crotonaldehyde), and dimers

and trimers of AcH will emerge, which significantly reduces the selectivity and yield of 3-HBA and makes it difficult to separate and purify the products [14]. Some researchers have also adopted the multi-phase catalytic method of AcH condensation, but the reaction temperature is relatively high (mostly above 100 °C), resulting in the continuous reaction of 3-HBA of the unstable structure, producing 2-butenal [10,13–16]. At the same time, the purification of 3-HBA among nonrecyclable catalysts and unreacted AcH is also a tough challenge [12,17]. More recently, it was found that basic ionic liquids were active for the aldol condensation reaction, which can achieve a higher total yield (75%) than NaOH (69%), while it is time-consuming and expensive [18]. Solid anion exchange resins were also tested in the aldol condensation of AcH, but the yield of 3-HBA was quite low over acrylic resin (5.5%) and microporous styrene resin (2.5%) [19]. It is of great importance to find a stable and efficient solid base catalyst for the synthesis of 3-HBA from AcH. Some researchers found that when different types of alkali are loaded on Al_2O_3, strong alkali sites can be generated after calcination, which shows good catalytic performance [14–16]. Furthermore, as 1,3-BDO is currently all imported, it is urgent to localize the production of 1,3-BDO. Therefore, it is of great significance to develop solid catalysts with stable performance and high selectivity and it is of great value to optimize the syntheses process of 3-HBA-1,3-BDO in order to make it environmentally friendly and inexpensive.

In this study, a series of MgO/Al_2O_3 composite acid–base solid catalysts are prepared through the coprecipitation method. Ca and La ions are introduced to modify the composite oxides. The catalytic activity is evaluated by a self-made tubular reactor. The catalytic performance of the modified MgO/Al_2O_3 solid catalyst is compared with that of the liquid catalyst (NaOH solution) to investigate the catalytic performance and lifespan of the modified MgO/Al_2O_3 for the synthesis of 3-HBA in AcH condensation.

2. Experimental

2.1. Preparation of Composite Oxide Catalysts

NaOH(≥99%), $Mg(NO_3)_2{\cdot}6H_2O$(≥99%), $Al(NO_3)_3{\cdot}9H_2O$(≥99%), $Ca(NO_3)_2{\cdot}4H_2O$(≥99%), $La(NO_3)_3{\cdot}6H_2O$(≥95%), and $NH_3{\cdot}H_2O$(28%) were purchased from Shanghai Aladdin Biochemical Technology Co., Ltd. CH_3CHO(≥30%) and CH_3CH_2OH(≥95%) were supplied by Jilin Petrochemical Company, Ltd., PetroChina. N_2(≥99%) and NH_3(≥99%) were purchased from Tianjin Ganda Gas Co., Ltd. and 46th Institute of China Electronics Technology Group Corporation. All the above chemicals were used as received without further purification.

$Al(NO_3)_3$ $9H_2O$ and $Mg(NO_3)_2$ $6H_2O$ were dissolved in deionized water to prepare a 1:1~4:1 ($MgO:Al_2O_3$) molar ratio of a magnesium nitrate and aluminum nitrate mixed solution. While the mixed solution was being stirred, an appropriate amount of ammonia was dropped into it, the pH was kept constant at 9~10, and then the reflux started. After that, the solution was heated to 100 ± 1 °C for 3~4 h. Afterward, the solution was cooled for 1–2 h and filtered, and the cake obtained was washed with abundant deionized water until pH 7. The filter cake was then dried in a vacuum oven at 80 °C for 24 h. After the filter cake was calcined at 500 °C for 3–6 h, the MgO/Al_2O_3 catalyst was obtained. The prepared MgO/Al_2O_3 was crushed and sieved, and the particles of 20~40 mesh size were selected. At room temperature, the particles were immersed in a certain concentration of $La(NO_3)_3$ or $Ca(NO_3)_2$ solution for 4~8 h in equal volume. After filtration, the filter cake was dried in a vacuum oven at 80 °C for 24 h and then calcined at 500 °C in an air atmosphere for 2 h to obtain Ca-MgO/Al_2O_3 or La-Ca-MgO/Al_2O_3.

2.2. Characterization of Composite Oxide Catalysts

The specific surface area and the pore size of the catalysts were measured by physical and chemical adsorption apparatus (BET, Autosorb-1-C, Anton Paar QuantaTec Inc.; Boynton Beach, FL, USA). The elemental composition was verified by Inductively Coupled Plasma-Optical Emission Spectrometry (ICP-OES, Agilent 725, Agilent Technologies Inc.; Santa Clara, CA, USA). The crystallinity of samples was characterized by an X-ray

diffractometer (XRD, Advance D8, Bruker Corporation; Billerica, MA, USA). Temperature-programmed desorption (TPD) was carried out using CO_2/NH_3 as probe molecules and was used to estimate the number and the intensity of acidity and alkalinity of samples by a chemical adsorption instrument (AutoChemII 2920, Micromeritics Inc., Norcross, GA, USA). Fourier-transform infrared spectroscopy (FTIR, AVATAR 360, Thermo Fisher Scientific Co., Ltd.; Waltham, MA, USA) was used to characterize the composites by pyridine adsorption infrared spectroscopy.

2.3. Evaluation of Catalyst Performances

The catalyst performance evaluation for the AcH condensation of composite oxide catalysts (MgO/Al_2O_3, Ca-MgO/Al_2O_3, and La-Ca-MgO/Al_2O_3) as well as a soluble catalyst (NaOH solution) were performed in a tubular reactor with 125 mm o.d. and 300 mm length.

Figure 1 depicts the catalyst performance evaluation device for the AcH condensation of composite oxide catalysts MgO/Al_2O_3, Ca-MgO/Al_2O_3, and La-Ca-MgO/Al_2O_3 in contrast with that of the soluble catalyst (NaOH solution). In a typical run, the reactor was loaded with quartz sand at the bottom and then filled with oxide catalyst (1.0 g, 20~40 mesh). Prior to reaction, the reactor was purged in situ for 1 h in 2000 cm^3/min dry N_2. The AcH in feed storage tank 1 was injected into the shell (composite oxide catalyst prefilled here) of tubular reactor 2 through plunger pump 4 at the rate of 1~10 mL/min. In the case of the soluble catalyst, the mixed solution NaOH (10 wt%) and AcH (30 wt%) in feed storage tank 1 was injected into tubular reactor 2 through plunger pump 4 at the rate of 1~10 mL/min. The reaction temperature was controlled to 0~30 °C through refrigerator 6. Adjusting the pressure of product receiving tank 5, the pressure in tubular reactor 2 was controlled. Both the tubular reactor and the product receiving tank were protected by nitrogen while starting up and shutting down. The reactants and products in the tubular reactor were both sampled by sampling valve 14 for subsequent analysis. The samples were identified and quantified by an Agilent Technologies 1260 Infinity II liquid chromatography system-based external calibration method. The chromatographic column type was TSK gel ODS-100S. The mobile phase consisted of 50% methanol and 50% deionized water. The analysis was conducted at the column temperature of 30 °C and injection volume of 20 μL. The running time was set to be 15 min at the flow rate of 0.7 mL/min.

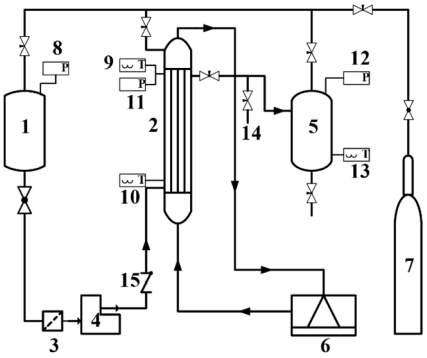

Figure 1. Schematic diagram of the experimental apparatus for catalytic performance evaluation. 1. AcH feed storage tank, 2. tubular reactor, 3. foot valve, 4. plunger pump, 5. product receiving tank, 6. refrigerating machine, 7. nitrogen cylinder, 8. pressure meter I, 9. thermometer I, 10. thermometer II, 11. pressure meter II, 12, pressure meter III, 13, thermometer III, 14, sampling valve, and 15. check valve.

The conversion is calculated based on AcH using Equation (1):

$$\text{Conversion} = \frac{C^0(\text{AcH}) - C^t(\text{AcH})}{C^0(\text{AcH})} \times 100\% \quad (1)$$

where C^0(AcH) is the AcH concentration in the feed line, and C^t(AcH) is the AcH on centration in the outlet stream at any time t.

The selectivity of objective products 3-HBA is calculated according to Equation (2):

$$\text{Selectivity (3-HBA)} = \frac{2C^t(\text{3-HBA})}{C^0(\text{AcH}) - C^t(\text{AcH})} \times 100\% \quad (2)$$

where C^t(3-HBA) is the 3-HBA concentration in the outlet stream at any time t.

3. Results and Discussion

First, in the catalyst performance experiment, the catalytic activity of different catalysts was compared to investigate the influence of loading elements and loading amount on the catalytic activity of AcH condensation, hence determining the appropriate loading amount. Subsequently, using ICP-OES, XRD, N_2 adsorption–desorption, BET, NH_3/CO_2-TPD, and pyridine adsorption infrared spectroscopy, the catalyst structure and the interaction between the oxides were characterized to determine the sources of alkali and acid active sites in the catalyst. Thirdly, the effects of reaction temperature, residence time, and reaction pressure on the AcH condensation reaction were investigated. Finally, the lifespan and deactivation reasons of the catalyst La-Ca-MgO/Al_2O_3 were studied and analyzed.

3.1. Characterization of Catalyst Performances

The activity of the NaOH solution and a series of composite oxide catalysts were investigated in the experimental device shown in Figure 1. The initial conditions of the AcH catalytic condensation reaction were as follows: AcH feed concentration 30%, reaction temperature 23 °C, residence time 70 min, and reaction pressure 200 kPa.

Table 1 indicates a high catalytic activity of the 20% NaOH solution. The conversion of AcH, and the selectivity and yield of 3-HBA reach 95.39%, 93.45%, and 89.14%, respectively. However, due to the large use of water and alkali solution in the reaction process, dilute H_2SO_4 or HCl had to be introduced for subsequent treatment to neutralize the system in acid and alkali, resulting in a large number of solid wastes Na_2SO_4 or NaCl, and causing great environmental pressure.

Table 1. Catalytic performance evaluation of composite oxides on AcH condensation.

$$CH_3{-}CHO \underset{}{\overset{\text{Cat.}}{\rightleftharpoons}} CH_3{-}\underset{\displaystyle OH}{\underset{|}{C}}H{-}CH_2{-}CHO \overset{\text{Cat.}}{\rightleftharpoons} CH_3{-}CH{=}CH{-}CHO + H_2O$$

NO.	Catalyst	Conversion of AcH/%	Selectivity of 3-HBA/%	Yield of 3-HBA/%
1	20%wt NaOH	95.39	93.45	89.14
2	MgO/Al_2O_3	64.13	86.42	55.42
3	2MgO/Al_2O_3	82.61	97.39	80.45
4	3MgO/Al_2O_3	88.23	85.38	75.33
5	4MgO/Al_2O_3	92.45	81.25	75.12
6	2.0%Ca-2MgO/Al_2O_3	84.83	77.43	65.68
7	2.3%Ca-2MgO/Al_2O_3	92.45	90.14	83.33
8	2.7%Ca-2MgO/Al_2O_3	88.50	82.92	73.38
9	3.0%Ca-2MgO/Al_2O_3	89.75	87.35	78.40
10	4.0%Ca-2MgO/Al_2O_3	90.17	85.42	77.02
11	0.1%La-2.3%Ca-2MgO/Al_2O_3	92.23	89.89	82.91
12	0.3%La-2.3%Ca-2MgO/Al_2O_3	94.19	90.43	85.18
13	0.5%La-2.3%Ca-2MgO/Al_2O_3	95.89	92.08	88.30
14	0.8%La-2.3%Ca-2MgO/Al_2O_3	92.53	89.10	82.44
15	1.0%La-2.3%Ca-2MgO/Al_2O_3	92.40	84.10	77.71

Note: 0.5%La-2.3%Ca-2MgO/Al_2O_3 indicates that the molar ratio of MgO to Al_2O_3 is 2:1; the level of La_2O_3 is 0.5 wt%; the level of CaO is 2.3 wt%.

Compared with the NaOH solution, the catalytic effect of the MgO/Al_2O_3 catalyst still has a certain gap. In most reactions, the conversion of raw materials and the selectivity and yield of target products have varying degrees of decline. With the increase in MgO content in the composite oxide, the catalytic effect is significantly improved. The conversion of AcH increases from 64.13 to 92.45%, and the yield of 3-HBA increases from 55.12 to 75.42%. Meanwhile, the selectivity of 3-HBA decreases from 97.39 to 81.25%. The decrease in selectivity leads to the increase in by-products, which makes the post-processing and separation of products far more difficult.

The introduction of Ca and La has an appreciable effect on the catalytic activity of the composite oxides. With the increase in Ca and La content, the conversion of raw materials and the selectivity and yield of the product increase first and then decrease. 0.5% La-2.3% Ca-$2MgO/Al_2O_3$ gives the best catalytic effect and possesses a conversion of 95.89%, somewhat better than those of the traditional catalyst NaOH solution. The selectivity and yield of the product are 92.08% and 88.3%, respectively, which is similar to the catalytic effect of the NaOH solution.

From the experimental results, the introduction of La-Ca makes a significant difference on the selectivity and conversion of the target product in the AcH condensation reaction. With the addition of La-Ca, the basicity of the catalyst can be strengthened and the mild reaction can be tempered, which avoids the continuous reaction of 3-HBA as a result of local overheating and promotes the selectivity of 3-HBA. On the other hand, the application of the tubular reactor in the reaction process is realized by replacing the homogeneous catalyst with a solid catalyst. Compared with the kettle reactor using the traditional homogeneous catalyst, the mass and heat transfer of the reaction system are significantly improved, which is also proven from the increase in raw material conversion.

3.2. Characterization of Catalyst Structure

Figure 2 describes the XRD patterns of composite oxides $2MgO/Al_2O_3$, 2.3%Ca-$2MgO/Al_2O_3$, and 0.5% La-2.3%Ca-$2MgO/Al_2O_3$. It can be seen that $2MgO/Al_2O_3$ shows characteristic bands of Al_2O_3 at 57°. Researchers have pointed out that when the calcination temperature is low, Al_2O_3 generally exists in the form of γ-Al_2O_3, so it is speculated that Al_2O_3 here basically exists in the form of γ-Al_2O_3, and characteristic bands of MgO appear at about 50° and 74°, indicating the formation of MgO crystal [20–22]. When Ca is introduced, characteristic bands of CaO appear at about 38°, indicating that calcium oxide has been loaded on the surface of the material [23,24]. When La is introduced again, characteristic bands of -La_2O_3 appear at about 24° and 29° [25]. The introduction of a small amount of La could change the acidity and alkalinity of the material. Combined with the experimental results of Table 1, the modified composite oxide 0.5% La-2.3% Ca-$2MgO/Al_2O_3$ shows good catalytic activity in the AcH condensation reaction. The conversion of AcH reaches 95.89%. The selectivity of 3-HBA is 92.08% and the yield is 88.30%. All these data demonstrate that the catalyst performs obviously better than that before modification.

Figure 3 represents the N_2 adsorption–desorption isotherms of $2MgO/Al_2O_3$, 2.3% Ca-$2MgO/Al_2O_3$, and 0.5% La-2.3% Ca-$2MgO/Al_2O_3$. It can be seen from Figure 3 that the three composites all exhibit type IV curves, showing an H1 hysteresis loop at higher pressure. It is analyzed that this phenomenon is caused by the capillary condensation of nitrogen in the pores of the composites, indicating that the prepared composites have an obvious mesoporous structure [26,27]. It can be seen from Table 2 that the contents of La, Ca, Mg, and Al match the theoretical ones in most cases. Otherwise, after the introduction of Ca and La ions, the specific surface area of the composites decreases from 322.8 m^2/g to about 280.9 m^2/g. The pore volume changes little, being maintained at about 0.44 cm^3/g. The pore size increases from 4.9 nm to 5.3 nm. According to the experimental results in Table 1, the increase in pore size is favorable to the catalytic condensation of AcH to synthesize 3-HBA. A larger pore size is conducive to the diffusion of 3-HBA from the pores

of the composites, which reduces the probability of continuous reaction to 2-butenal, thus improving the selectivity of 3-HBA.

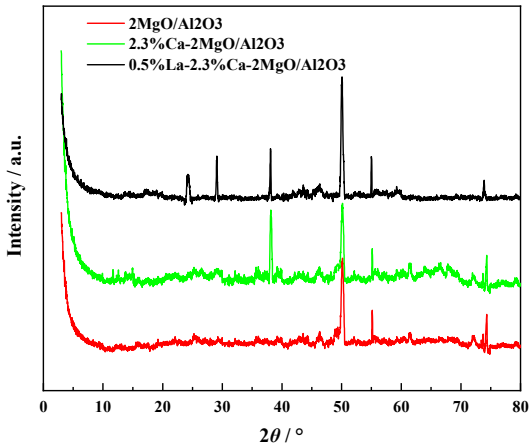

Figure 2. XRD patterns of composite oxides.

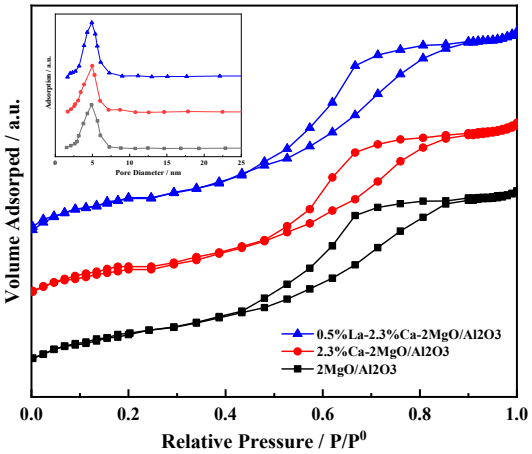

Figure 3. N_2 adsorption–desorption isotherms of composite oxides.

Table 2. Structural properties of composite oxides.

Composite Oxides	$MgO:Al_2O_3$(ICP)	CaO/wt%(ICP)	La_2O_3/wt%(ICP)	Specific Surface Area/m^2/g	Pore Volume/cm^3/g	Pore Size/nm
$2MgO/Al_2O_3$	2.11:1	0	0	322.8	0.46	4.9
$2.3\%Ca\text{-}2MgO/Al_2O_3$	2.17:1	2.42	0	285.3	0.45	5.2
$0.5\%La\text{-}2.3\%Ca\text{-}2MgO/Al_2O_3$	2.09:1	2.39	0.44	280.9	0.44	5.3

Figures 4 and 5 show the CO_2-TPD and NH_3-TPD spectra of the composite oxides $2MgO/Al_2O_3$, $2.3\%Ca\text{-}2MgO/Al_2O_3$, and $0.5\%La\text{-}2.3\%Ca\text{-}2MgO/Al_2O_3$, respectively. The total basicity/acidity listed in Table 3 was estimated from the area below the TPD curve due to CO_2/NH_3 desorption by using calibration from a known amount of CO_2/NH_3 decomposition in helium flow (25 mL/min). The CO_2/NH_3-TPD profiles of $0.5\%La\text{-}2.3\%Ca\text{-}2MgO/Al_2O_3$ were deconvoluted by using the Gaussian multipeak fitting function built into Origin7.5 software.

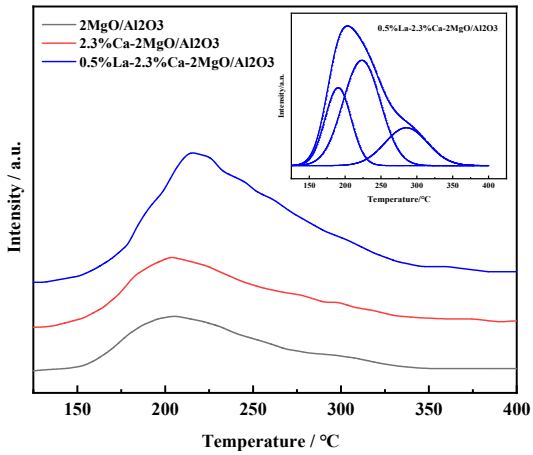

Figure 4. CO_2-TPD profiles of composite oxides.

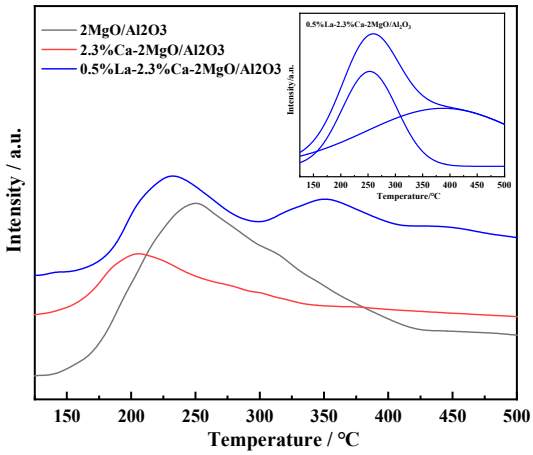

Figure 5. NH_3-TPD profiles of composite oxides.

Table 3. Acid/Base properties of composite oxides.

Composite Oxides	$2MgO/Al_2O_3$	2.3%Ca-$2MgO/Al_2O_3$	0.5%La-2.3%Ca-$2MgO/Al_2O_3$
total alkali content/mmol/g	0.135	0.157	0.916
total acid content/mmol/g	0.574	0.391	0.413
T1(150~250 °C)	0.052	0.038	0.209
T2(250~320 °C)	0.357	0.287	0.031
T3(320~500 °C)	0.165	0.066	0.173

According to the study of Garbarino [28], there are at least three kinds of acidic sites on the surface of Al_2O_3, namely, weak acidic sites at 150 °C~250 °C, medium-strong acidic sites at 250~320 °C, and strong acidic sites at 320~500 °C. Comprehensive analysis of Figure 5 and Table 3 finds that the introduction of Ca ions significantly reduces the number of strong acid sites on the surface of $2MgO/Al_2O_3$, while the introduction of La ions slightly increases the number of strong acid sites on the surface of 2.3%Ca-$2MgO/Al_2O_3$. Bao et al. studied the aldol condensation of methyl acetate with formaldehyde over a Ba-La/Al_2O_3 catalyst. They found that a decrease in surface acidity not only inhibited the formation of coke but also improved the catalytic activity [29–31]. The experimental data listed in Table 1 also show that the decreases in surface acidity probably has negative effects on selectivity, but it has a significant promoting effect on improving AcH conversion and 3-HBA yield.

In addition, the broad peaks can be deconvoluted into a desorption of CO_2 on the weak (peak below 300 °C), medium (peak between 300 °C and 450 °C), and strong basic sites (peak above 450 °C) [32,33]. As shown in Figure 4, on the surfaces of 0.5% La-2.3% Ca-2MgO/Al_2O_3, there exists several weakly alkaline sites corresponding to a desorption temperature below 300 °C. After the introduction of Ca ions, the number of alkaline sites increases on the surface of 2MgO/Al_2O_3. When La ions are introduced, not only do alkaline sites on the surface of 2MgO/Al_2O_3 composites increase in number, but the strength of alkaline sites is also enhanced. Combined with Figures 2 and 4 and Figure 5, it is shown that the introduction of Ca and La changes the surface properties of 2MgO/Al_2O_3. After the introduction of Ca, the number of acid sites on the surface of 2.3%Ca-2MgO/Al_2O_3 decreases slightly while the total alkali contents increase significantly. When La is introduced into 2.3% Ca-2MgO/Al_2O_3, the total amount of alkali increases greatly and the total amount of acid slightly increases. The final effect is reflected in the experimental results of the AcH catalytic condensation reaction given in Table 1. The use of the 0.5% La-2.3% Ca-2MgO/Al_2O_3 catalyst improves the conversion, which shows that the suitable surface of the catalyst is beneficial to improve the conversion of raw materials.

Figure 6 elaborates the pyridine adsorption infrared characterization of composite oxides 2MgO/Al_2O_3, 2.3% Ca-2MgO/Al_2O_3, and 0.5% La-2.3% Ca-2MgO/Al_2O_3. It is used to evaluate the strength and types of acid sites of the composite oxides.

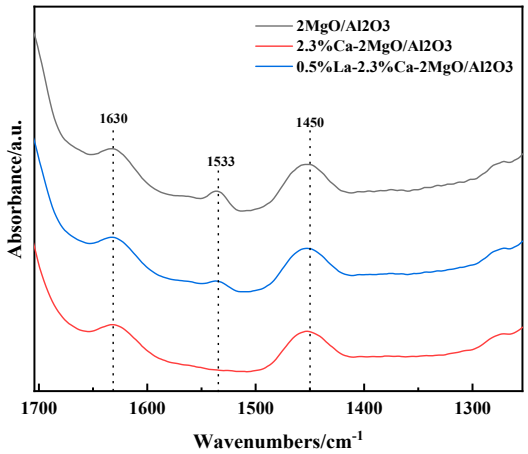

Figure 6. Py-IR spectra of composite oxides.

It can be seen from Figure 6 that the spectra of pyridine adsorbed on composite oxides 2MgO/Al_2O_3, 2.3% Ca-2MgO/Al_2O_3, and 0.5% La-2.3% Ca-2MgO/Al_2O_3 displaying bands around 1450 cm^{-1}, 1533 cm^{-1}, and 1630 cm^{-1} are assigned to pyridine coordinated to Lewis acid sites [34–36]. In Figure 6, no characteristic bands of the interaction between the Bronsted acid site and pyridine ring are found at 1545 cm^{-1}, indicating that the surface of the prepared composite oxides is mainly a Lewis acid site [37,38]. With the introduction of Ca-La ions, it is obvious that the characteristic bands at 1533 cm^{-1} is weakened, which reduces the number of Lewis acid sites on the surface of 2MgO/Al_2O_3. This is consistent with the results shown in Table 3 and Figure 5. This may be the result of the interaction between the oxide formed by Ca-La and the acid sites on the surface of 2MgO/Al_2O_3 or the coverage of the acid sites on the surface of 2MgO/Al_2O_3. In accordance with the experimental results of Table 1, the reduction in Lewis acid sites helps to improve the conversion of AcH, as well as the selectivity and yield of the 3-HBA.

3.3. The Effect of Process Condition on Catalyst Performances

The catalytic performance of 0.5% La-2.3% Ca-2MgO/Al_2O_3 in the catalytic condensation of AcH to 3-HBA is studied by a single-factor experiment on the catalyst activity characterization device shown in Figure 1. The effects of reaction temperature, residence

time, and reaction pressure on AcH conversion, as well as selectivity and yield of 3-HBA, are investigated.

3.3.1. The Effect of Reaction Temperature on Catalyst Performances

When the feed concentration of AcH is 30%, the residence time is 70 min, and the reaction pressure is 200 kPa, the effect of temperature on the synthesis of 3-HBA by AcH condensation is investigated. The experimental results are shown in Figure 7.

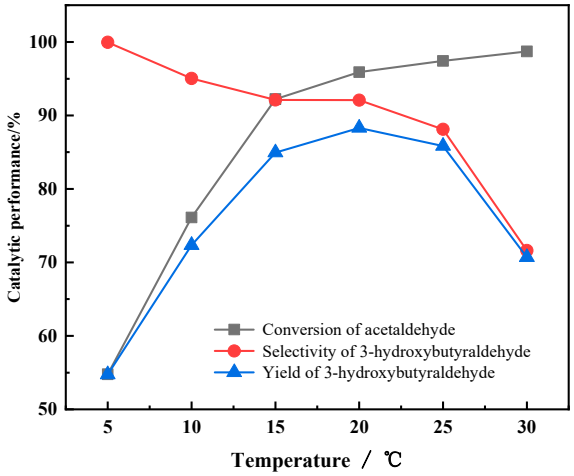

Figure 7. Effect of reaction temperature on AcH condensation.

It can be seen from Figure 7 that under the action of the 0.5% La-2.3% Ca-2MgO/Al_2O_3 catalyst, the conversion of AcH and the yield of 3-HBA are very low at 5 °C, indicating that most AcH does not participate in the reaction. With the increase in temperature, the conversion of AcH and the yield of 3-HBA increase remarkably, and the selectivity of 3-HBA decreases slightly. When the reaction temperature reaches 20 °C, the conversion of AcH increases to 95.89%, and the selectivity and yield of 3-HBA are 92.08% and 88.30%, respectively. The selectivity and yield of 3-HBA decrease with the increase in reaction temperature, although the conversion of AcH continues to grow, manifesting that the reaction temperature is too high. Under the action of 0.5% La-2.3% Ca-2MgO/Al_2O_3, part of the synthesized 3-HBA continues to react to form 2-butenal or tripolymerized AcH. Thereupon, although the conversion of AcH remains high, the selectivity of the target product decreases, which results in poor yield.

3.3.2. The Effect of Residence Time on Catalyst Performances

When the feed concentration of AcH is 30%, the reaction temperature is 20 °C, and the reaction pressure is 200 kPa, the effect of reaction residence time on the synthesis of 3-HBA by AcH condensation is investigated.

It can be seen from Figure 8 that under the action of the 0.5% La-2.3% Ca-2MgO/Al_2O_3 catalyst, when the residence time increases from 40 min to 120 min, the conversion of AcH increases from 83.63 to 97.33%, indicating that most AcH is involved in the reaction. The selectivity and yield of 3-HBA first increase and then decrease. When the residence time increases from 40 min to 70 min, the selectivity and yield of 3-HBA increase from 66.44% and 55.56% to 92.08% and 88.30%, respectively. With the increase in residence time, the selectivity and yield decrease to 79.07% and 76.96%, respectively. Analyzing the reason, it is found that at the reaction temperature of 20 °C, a longer residence time leads to the continuous reaction of 3-HBA. Considering the conversion of AcH as well as selectivity and yield of 3-HBA, the suitable residence time is 70 min.

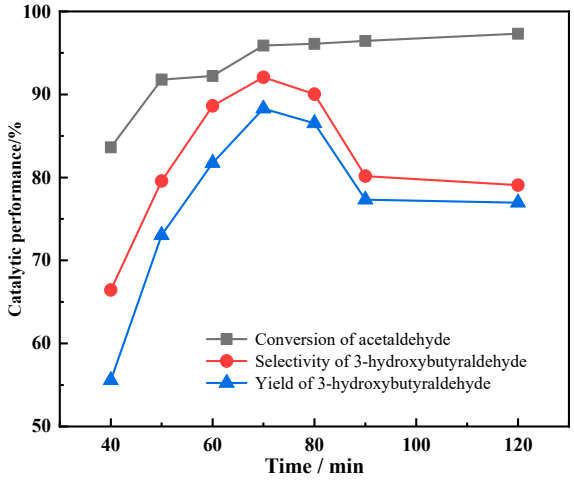

Figure 8. Effect of residence time on AcH condensation.

3.3.3. The Effect of Reaction Pressure on Catalyst Performances

When the concentration of AcH is 30%, the reaction temperature is 20 °C, and the residence time is 70 min, the effect of reaction pressure on the synthesis of 3-HBA by AcH condensation is investigated.

It can be seen from Figure 9 that when 0.5% La-2.3% Ca-2MgO/Al_2O_3 is used as the catalyst for the AcH condensation reaction, the conversion and the selectivity are relatively low at 100 kPa. This may be due to the fact that the boiling point of AcH is 20.8 °C under this pressure condition, and the reaction temperature is 20 °C. Due to the local overheating in the liquid phase, some AcH is vaporized and then enters into the gas phase. The decrease in the concentration of AcH in the liquid phase significantly reduces the conversion and yield, which also indicates that the presence of AcH gas in the reactor has no positive effect on the catalytic reaction. The contact between reactants is mainly liquid–solid contact. Both the boiling point of AcH and the concentration of AcH in the liquid phase increase with the increase in the reaction pressure. The conversion of AcH and yield also increase noticeably with the increase in reaction pressure. When the reaction pressure continues to increase, the conversion of AcH and the selectivity of 3-HBA hardly change. In order to maintain the reaction system in a liquid phase, the reaction pressure is selected as 200 kPa.

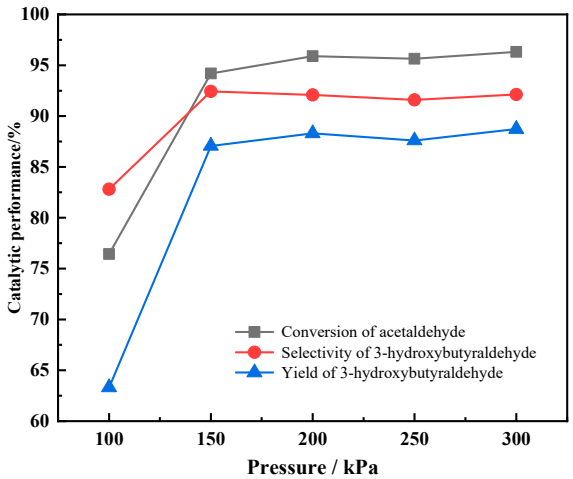

Figure 9. Effect of reaction pressure on AcH condensation.

3.4. Catalyst Lifespan and Regeneration

The lifespan of the 0.5% La-2.3% Ca-2MgO/Al_2O_3 catalyst is investigated under the conditions of 30% AcH feed concentration, 20 °C reaction temperature, 70 min residence time, and 200 kPa reaction pressure.

It can be seen from Figure 10 that the catalytic activity of 0.5% La-2.3% Ca-2MgO/Al_2O_3 is relatively high within 5 h. The conversion of AcH is above 95%, and the selectivity and yield of 3-HBA are also maintained at above 90% and 85%, respectively. With the increase in the operation time of the device, the selectivity and yield of 3-HBA decrease, but the conversion of AcH remains above 90%. This may be due to the long diffusion time of 3-HBA due to carbon deposition in the pores of the composite at this time, resulting in continuous reaction to produce 2-butenal. Some researchers also studied the causes of catalytic deactivation in a relatively low-temperature reaction. They found that the formation of carbon deposits led to the catalytic deactivation. The used catalyst contained a significant amount of carbon (14.9 wt%), while the precursor only contained 2 wt% [39,40]. In addition, the presence of impurities in the reactants or the formation of inactive metal hydroxides by by-product H_2O may probably reduce the activity of the catalyst.

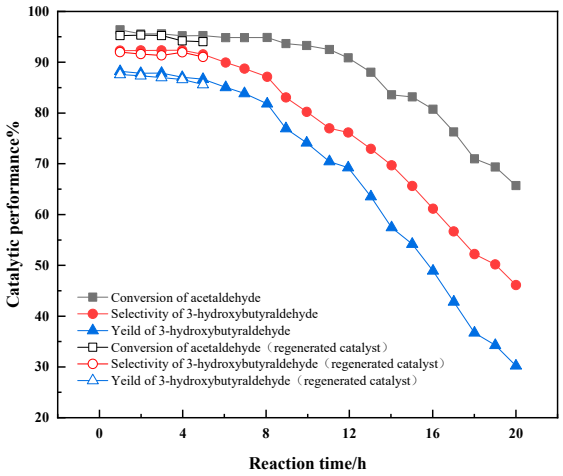

Figure 10. Lifetime of composite oxides 0.5%La-2.3%Ca-2MgO/Al_2O_3.

With the increase in operation time, the conversion of AcH and the selectivity and yield of 3-HBA reduce significantly. It is possible that the reactants cover most of the catalyst surface with alkaline sites, preventing the diffusion of AcH to the catalyst surface, thus making some AcH dimers or even trimers. At 20 h, the yield of the product reduces to less than 30%.

Based on previous studies, the deactivated catalyst was regenerated (500 °C; 2 h) and put into the reaction system again. The results are shown in Figure 10. Compared with the fresh catalyst, the catalytic activity of the regenerated catalyst does not show a significant downward trend, and no irreversible deactivation such as structural damage and loss of active components is found. The catalyst could be burned completely at 500 °C for 2 h to recover the catalytic activity well, which could realize the continuous operation of the catalytic condensation reaction.

4. Conclusions

(1) A series of composite oxides 2MgO/Al_2O_3 are prepared by the co-precipitation method. Ca and La ions are introduced and applied to the catalytic condensation of AcH to synthesize 3-HBA. The catalytic activity of the composite materials is significantly improved. The catalyst performance of 0.5% La-2.3% Ca-2MgO/Al_2O_3 is better than those of other composite oxides used in the study. Under the conditions of an AcH content of 30%, reaction temperature of 23 °C, reaction time of 70 min, and reaction pressure of 200 kPa, the conversion of AcH reaches 95.89%, the selectivity of 3-HBA is 92.08%, and the yield is 88.30%.

(2) The characterization of process conditions shows that reaction temperature has a significant effect on the selectivity of the product due to the fact that the aldol conden-

sation of AcH is an exothermic process and the transformation of AcH is unfavorable at higher temperature.

(3) The characterization results show that after the introduction of Ca and La ions into the composite oxide $2MgO/Al_2O_3$, the acid and alkaline sites on the surface are significantly improved and optimized, but the surface area of the material decreases and the pore size increases. It is beneficial to the reaction from the perspective of the catalytic condensation of AcH to 3-HBA.

(4) The investigation on the catalytic lifespan of 0.5% La-2.3% Ca-$2MgO/Al_2O_3$ shows that within 5 h, the conversion of AcH and the selectivity and yield of 3-HBA are high, and the catalytic activity recovers well after regeneration. Under the same process conditions, the catalytic performance of the composite oxide is equivalent to that of the traditional liquid alkaline catalyst, and it is environmentally friendly. Therefore, it is feasible and has broad prospects in industrial application to use this catalyst for the catalytic condensation of AcH to synthesize 3-HBA.

Author Contributions: Data curation, H.R.; funding acquisition, W.L.; investigation, H.R.; methodology, W.L.; project administration, W.L.; resources, W.L.; writing—original draft, H.R. All authors have read and agreed to the published version of the manuscript.

Funding: This research received no external funding.

Institutional Review Board Statement: Not applicable.

Informed Consent Statement: Not applicable.

Conflicts of Interest: The authors declare no conflict of interest.

References

1. Abdel-Rahem, R.A. Influence of 1,3-Butanediol on the viscoelasticity of surfactant solutions. *J. Surfact. Deterg.* **2014**, *17*, 353–362. [CrossRef]
2. Azarang, N.; Movagharnejad, K.; Pirdashti, M.; Ketabi, M. Densities, viscosities, and refractive indices of poly(ethylene glycol) 300 + 1,2-Ethanediol, 1,2-Propanediol, 1,3-Propanediol, 1,3-Butanediol, or 1,4-Butanediol binary liquid mixtures. *J. Chem. Eng. Data* **2020**, *65*, 3448–3462. [CrossRef]
3. Zhu, Y.; Cheng, X.; Pang, X.; Yu, L. Heterotactic enthalpic interactions of L-Arginine and L-Proline with 1,3-Butanediol and 2,3-Butanediol in aqueous solutions. *J. Chem. Eng. Data* **2010**, *55*, 3813–3816. [CrossRef]
4. Zhang, Z.; Wang, Y.; Lu, J.; Zhang, C.; Wang, M.; Li, M.; Liu, X.; Wang, F. Conversion of isobutene and formaldehyde to diol using praseodymium-doped CeO_2 catalyst. *ACS Catal.* **2016**, *6*, 8248–8254. [CrossRef]
5. Song, H.; Tang, Z.; Chen, J. Prins condensation of formaldehyde with alkene using functional acid ionic liquid as catalyst. *J. Mol. Catal.* **2008**, *22*, 403–407.
6. Windhorst, K.A.; Cortez, O. 1,3-Butylene Glycl with Reduced Odor. U.S. Patent US8445733B1, 21 May 2013.
7. Tsuji, Y.; Tagawa, K. 1,3-Butylene Glygol of High Purity and Method for Producing the Same. U.S. Patent US6376725B1, 23 April 2002.
8. Matsuyama, A.; Yamamoto, H.; Kawada, N.; Kobayashi, Y. Industrial Production of (R)-1,3-Butanediol by new biocatalysts. *J. Mol. Catal. B Enzym.* **2001**, *11*, 513–521. [CrossRef]
9. Iwata, M.; Yazaki, R.; Suzuki, Y.; Kumagai, N.; Shibasaki, M. Direct catalytic asymmetric aldol reactions of thioamides: Toward a stereo controlled synthesis of 1,3-Polyols. *J. Am. Chem. Soc.* **2009**, *131*, 18244–18245. [CrossRef]
10. Young, D.Z.; Hanspal, S.; Davis, J.R. Aldol condensation of acetaldehyde over titania, hydroxyapatite, and magnesia. *ACS Catal.* **2016**, *6*, 3193–3202. [CrossRef]
11. Rekoske, J.E.; Barteau, M.A. Kinetics, selectivity, and deactivation in the aldol condensation of acetaldehyde on anatase titanium dioxide. *Ind. Eng. Chem. Res.* **2011**, *50*, 41–51. [CrossRef]
12. Yan, T.; Yao, S.; Dai, W.; Wu, G.; Guan, N.; Li, L. Self-aldol condensation of aldehydes over Lewis acidic rare-earth cations stabilized by zeolites. *Chin. J. Catal.* **2021**, *42*, 595–605. [CrossRef]
13. Barrett, C.J.; Chheda, J.N.; Huber, G.W.; Dumesic, J.A. Single-reactor process for sequential aldol-condensation and hydrogenation of biomass-derived compounds in water. *Appl. Catal. B* **2006**, *66*, 111–118. [CrossRef]
14. Valihura, K.V.; Larina, O.V.; Kyriienko, P.I.; Balakin, D.Y.; Soloviev, S.O. Influence of modifying additives of Lanthanum and Cerium oxides on Acid-Base characteristics and catalytic properties of MgO-Al_2O_3 systems in the processes of gas-phase conversion of ethanol to 1-butanol. *Theor. Exp. Chem.* **2021**, *56*, 404–411. [CrossRef]
15. Singh, M.; Zhou, N.; Dilip, K.P.; Klabunde, K.J. IR Spectral evidence of aldol condensation: Acetaldehyde adsorption over TiO_2 surface. *J. Catal.* **2008**, *260*, 371–379. [CrossRef]

16. Kagunya, W.; Jones, W. Aldol condensation of acetaldehyde using calcined layered double hydroxides. *Appl. Clay Sci.* **1995**, *10*, 95–102. [CrossRef]
17. Korolova, V.; Kikhtyanin, O.; Veselý, M.; Vrtiška, D.; Paterová, I.; Fíla, V.; Čapek, L.; Kubička, D. On the Effect of the M^{3+} Origin on the Properties and Aldol Condensation Performance of MgM^{3+} Hydrotalcites and Mixed Oxides. *Catalysts* **2021**, *11*, 992–1008. [CrossRef]
18. McNeice, P.; Marr, P.C.; Marr, A.C. Basic ionic liquids for catalysis: The road to greater stability. *Catal. Sci. Technol.* **2021**, *11*, 726–741. [CrossRef]
19. Wu, Y.H.; Ren, W.H.; Liang, Z.L.; Liu, Z.N.; Wu, G.S. Liquid-phase aldol condensation of AcH and its kinetics. *Chem. React. Eng. Technol.* **2013**, *29*, 75–80.
20. Evangelista, J.P.D.C.; Gondimm, A.D.; Di Souza, L.; Araujo, A.S. Alumina-supported Potassium compounds as heterogeneous catalysts for biodiesel production: A Review. *Renew. Sustain. Energy Rev.* **2016**, *59*, 887–894. [CrossRef]
21. Xie, W.; Chen, J. Heterogeneous interesterification of triacylglycerols catalyzed by using Potassium-doped Alumina as a solid catalyst. *J. Agric. Food Chem.* **2014**, *62*, 10414–10421. [CrossRef]
22. Fang, P.; He, M.; Xie, Y.; Luo, M.F. XRD and Raman Spectroscopic comparative study on phase transformation of γ-Al_2O_3 at high temperature. *Spectrosc. Spectr. Anal.* **2006**, *11*, 2039–2042.
23. Khemthong, P.; Luadthong, C.; Nualpaeng, W.; Changsuwan, P.; Tongprem, P.; Viriya-Empikul, N.; Faungnawakij, K. Industrial eggshell wastes as the heterogeneous catalysts for microwave-assisted biodiesel production. *Catal. Today* **2012**, *190*, 112–116. [CrossRef]
24. Kumar, V.S.; Lee, Z.H.; Sim, J.H.; Law, S.C.; Mohamed, A.R. Improved CO_2 Sorption Performance of Calcium Oxide (CaO) Sorbent with Nickel Oxide. *Earth Environ. Sci.* **2019**, *268*, 012026.
25. Maheshwaran, G.; Muneeswari, R.S.; Bharathi, A.N.; Kumar, M.K.; Sudhahar, S. Eco-friendly synthesis of lanthanum oxide nanoparticles by Eucalyptus globulus leaf extracts for effective biomedical applications. *Mater. Lett.* **2021**, *283*, 128799. [CrossRef]
26. Bang, Y.; Park, S.; Han, S.J.; Yoo, J.; Song, J.H.; Choi, J.H.; Kang, K.H.; Song, I.K. Hydrogen Production by Steam Reforming of liquefied Natural Gas (LNG) over mesoporous Ni/Al_2O_3 catalyst prepared by an EDTA-assisted impregnation method. *Appl. Catal. B* **2016**, *180*, 179–188. [CrossRef]
27. Kikhtyanin, O.; Čapek, L.; Smoláková, L.; Tišler, Z.; Kadlec, D.; Lhotka, M.; Diblíková, P.; Kubička, D. Influence of Mg-Al mixed oxide compositions on their properties and performance in aldol Condensation. *Ind. Eng. Chem. Res.* **2017**, *56*, 13411–13422. [CrossRef]
28. Garbarino, G.; Wang, C.; Valsamakis, I.; Chitsazan, S.; Riani, P.; Finocchio, E.; Flytzani-Stephanopoulos, M.; Busca, G. Acido-basicity of lanthana/alumina catalysts and their activity in ethanol conversion. *Appl. Catal. B Environ.* **2017**, *200*, 458–468. [CrossRef]
29. Bao, Q.; Zhu, W.; Yan, J.; Zhang, C.; Ning, C.; Zhang, Y.; Hao, M.; Wang, Z. Vapor phase aldol condensation of methyl acetate with formaldehyde over a $Ba–La/Al_2O_3$ catalyst: The stabilizing role of La and effect of acid–base properties. *RSC Adv.* **2017**, *7*, 52304. [CrossRef]
30. Bao, Q.; Bu, T.; Yan, J.; Zhang, C.; Ning, C.; Zhang, Y.; Hao, M.; Zhang, W.; Wang, Z. Synthesis of Methyl Acrylate by Aldol Condensation of Methyl Acetate with Formaldehyde Over Al_2O_3-Supported Barium Catalyst. *Catal. Lett.* **2017**, *147*, 1540–1550. [CrossRef]
31. Bai, S.; Dai, Q.; Chu, X.; Wang, X. Dehydrochlorination of 1,2-dichloroethane over Ba-modified Al_2O_3 catalysts. *RSC Adv.* **2016**, *6*, 52564–52574. [CrossRef]
32. Wang, Y.; Li, H.X.; Li, X.G.; Xiao, W.D.; Chen, D. Hydrogenation of CO to olefins over a supported iron catalyst on $MgAl_2O_4$ spinel: Effects of the spinel synthesis method. *RSC Adv.* **2020**, *10*, 40815–40829. [CrossRef]
33. Wang, K.; Miao, C.; Liu, Y.; Cai, L.; Jones, W.; Fan, J.; Li, D.; Feng, J. Vacancy enriched ultrathin TiMgAl-layered double hydroxide/graphene oxides composites as highly efficient visible-light catalysts for CO_2 reduction. *Appl. Catal. B Environ.* **2020**, *270*, 118878. [CrossRef]
34. Chen, L.F.; Noreña, L.E.; Navarrete, J.; Wang, J.A. Improvement of surface acidity and structural regularity of Zr-modified mesoporous MCM-41. *Mater. Chem. Phys.* **2006**, *97*, 236–242. [CrossRef]
35. Zhang, Y.Q.; Wang, S.J.; Wang, J.W.; Lou, L.L.; Zhang, C.; Liu, S. Synthesis and characterization of Zr-SBA-15 supported tungsten oxide as a new mesoporous solid acid. *Solid State Sci.* **2009**, *11*, 1412–1418. [CrossRef]
36. Jia, A.; Li, J.; Zhang, Y.; Song, Y.; Liu, S. Synthesis and characterization of nanosized micromesoporous $Zr–SiO_2$ via ionic liquid templating. *Mater. Sci. Eng.* **2009**, *28*, 1217–1226. [CrossRef]
37. Hernández-Giménez, A.M.; Ruiz-Martínez, J.; Puértolas, B.; Pérez-Ramírez, J.; Bruijnincx, P.C.; Weckhuysen, B.M. Operando Spectroscopy of the Gas-Phase Aldol Condensation of Propanal over Solid Base Catalysts. *Top. Catal.* **2017**, *60*, 1522–1536. [CrossRef]
38. Parry, E. An infrared study of pyridine adsorbed on acidic solids characterization of surface acidity. *J. Catal.* **1963**, *2*, 371. [CrossRef]
39. Tišler, Z.; Vondrová, P.; Hrachovcová, K.; Štěpánek, K.; Velvarská, R.; Kocík, J.; Svobodová, E. Aldol Condensation of Cyclohexanone and Furfural in Fixed-Bed Reactor. *Catalysts* **2019**, *9*, 1068. [CrossRef]
40. Vrbková, E.; Tišler, Z.; Vyskočilová, E.; Kadlec, D.; Červený, L. Aldol Condensation of Benzaldehyde and Heptanal: A Comparative Study of Laboratory and Industrially Prepared Mg-Al Mixed Oxides. *Chem. Technol. Biotechnol.* **2017**, *93*, 166–173. [CrossRef]